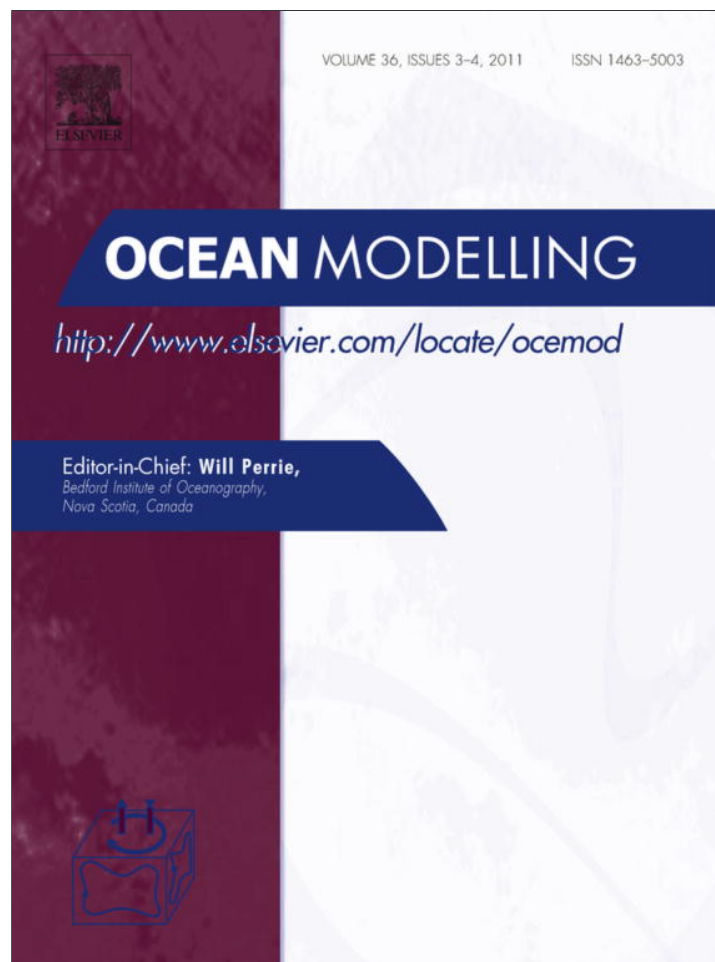


Provided for non-commercial research and education use.
Not for reproduction, distribution or commercial use.



This article appeared in a journal published by Elsevier. The attached copy is furnished to the author for internal non-commercial research and education use, including for instruction at the authors institution and sharing with colleagues.

Other uses, including reproduction and distribution, or selling or licensing copies, or posting to personal, institutional or third party websites are prohibited.

In most cases authors are permitted to post their version of the article (e.g. in Word or Tex form) to their personal website or institutional repository. Authors requiring further information regarding Elsevier's archiving and manuscript policies are encouraged to visit:

<http://www.elsevier.com/copyright>



Contents lists available at ScienceDirect

Ocean Modelling

journal homepage: www.elsevier.com/locate/ocemod

Model initialization in a tidally energetic regime: A dynamically adjusted objective analysis

Alfredo L. Aretxabaleta^{a,*}, Keston W. Smith^b, Dennis J. McGillicuddy Jr.^b, Joaquim Ballabrera-Poy^c

^a Institut de Ciències del Mar – CSIC, Barcelona, Spain

^b Woods Hole Oceanographic Institution, Woods Hole, MA, USA

^c Unidad de Tecnología Marina – CSIC, Barcelona, Spain

ARTICLE INFO

Article history:

Received 2 March 2010

Received in revised form 13 November 2010

Accepted 2 January 2011

Available online 18 January 2011

Keywords:

Model initialization

Hydrographic skill

Objective analysis

Data assimilation

ABSTRACT

A simple improvement to objective analysis of hydrographic data is proposed to eliminate spatial aliasing effects in tidally energetic regions. The proposed method consists of the evaluation of anomalies from observations with respect to circulation model fields. The procedure is run iteratively to achieve convergence. The method is applied in the Bay of Fundy and compared with traditional objective analysis procedures and dynamically adjusted climatological fields. The hydrographic skill (difference between observed and model temperature and salinity) of the dynamically adjusted objective analysis is significantly improved by reducing bias and correcting the vertical structure. Representation of the observed velocities is also improved. The resulting flow is consistent with the known circulation in the Bay.

© 2011 Elsevier Ltd. All rights reserved.

1. Introduction

Initialization of ocean circulation models remains a challenge for both coastal and large-scale ocean simulations. Several approaches have been used in the past to improve the skill of initialization products: using climatological hydrographic fields (Ezer and Mellor, 1994; Danabasoglu et al., 1996), nudging temperature and salinity observations into model solutions (Malanotte-Rizzoli and Holland, 1986), using objective analysis of observations to generate updated fields (Robinson et al., 1989, 1996), developing various types of inverse methods as Kalman Filters (Fukumori et al., 1993; Ballabrera-Poy et al., 2001) and adjoint methods (Marotzke and Wunsch, 1993; Kleeman et al., 1995). The appropriateness of each method depends on the associated goals and available resources. The use of climatological initialization could require long integrations (even thousands of years) so that model dynamics and exterior forcings drive model solutions toward equilibrium (McWilliams, 1996). The climatological approach is usually preferred in large scale ocean studies that require long spin-ups. Although climatological fields can be useful for general and process studies, more realistic initial conditions are necessary for event and hindcast/forecast studies. The simplest approach is to embed observations into the model mass field using nudging. A more elaborate approach is to calculate anomalies between observations and climatological background fields and objectively analyze those

anomalies. Finally, a more computationally expensive approach is to produce initial conditions with adjoint methods or ensemble smoother simulations.

Herein we describe an improvement of the traditional objective analysis technique to include dynamical effects. Instead of calculating the anomalies (departures of the observations from a reference field) with respect to a climatological background, we compute the anomaly as the difference between observations and the model solution at the time of the observation. Applications of this dynamically adjusted objective analysis have been used in atmospheric (Goerss and Phoebus, 1993; Lorenc et al., 2000) and oceanographic applications (Carton et al., 2000b; Stammer et al., 2000). In the current study an iterative approach is used to improve skill and computational performance. The method is applied in the Gulf of Maine/Bay of Fundy Region (Fig. 1).

The Gulf of Maine and Bay of Fundy have been intensely studied for decades using observations and model simulations. Buoyancy-driven flows, winds, and tides control the circulation of the Gulf and the adjacent Bay (Bigelow, 1927; Brooks, 1985; Brooks and Townsend, 1989). The main characteristic of the Bay is the presence of some of the world's largest tides, especially the M_2 tidal constituent, with tidal ranges of up to 8 m at the mouth and 16 m at the head of the Bay (Garrett, 1972; Greenberg, 1983). Tidal rectification dominates the resulting residual circulation with flow into the Bay along the Nova Scotia shelf and outflow along the coast of New Brunswick and Grand Manan Island (Bigelow, 1927; Greenberg, 1983). The presence of cyclonic circulation near the mouth of the Bay, caused by the combination of tidal rectification

* Corresponding author. Tel.: +34 93 230 9500.

E-mail address: alfredo@icm.csic.es (A.L. Aretxabaleta).

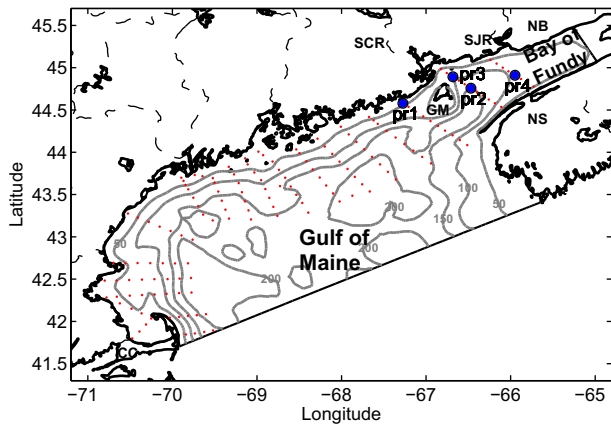


Fig. 1. Map of the study region showing the model domain of the Gulf of Maine and Bay of Fundy. Small red dots indicate the horizontal position of the temperature and salinity observations. The blue dots indicate the positions of selected representative observations. The two main rivers near the Bay of Fundy are indicated with thin dashed lines: St. Croix (SCR) and St. John (SJR). The bottom topography contours of 50, 100, 150, and 200 m are indicated. (GM – Grand Manan Island; NS – Nova Scotia; NB – New Brunswick; CC – Cape Cod).

and a dense water pool in the center of the Grand Manan basin, forms a persistent gyre with significant implications for the physics and biology of the region (Aretxabaleta et al., 2008, 2009). Additionally, the seasonally varying river discharge from the St. John River (Brooks, 1994; Bisagni et al., 1996) influences the near-surface hydrographic structure in the western and southern Bay. In this study we focus in the June 2006 period for which observations were available from cruises and moorings. Aretxabaleta et al. (2009) described a relatively strong Bay of Fundy gyre during June 2006 due to the presence of denser water near the bottom (compared with previous years and climatological densities).

In such an energetic regime as the Bay of Fundy with tidal excursions on the order of 15–25 km, hydrographic stations conducted during cruise surveys (usually lasting longer than a week) are subject to large tidal aliasing. The density gradients estimated from the observations introduce significant misrepresentations of actual density gradients, for instance when one transect is measured during ebb tide while the following one is conducted during flood tide. Here we introduce a method for dynamically adjusted objective analysis that significantly improves the skill of initialization products in regimes with large tidal excursions or in the proximity of frontal regions.

2. Data

One hundred and fifty hydrographic stations, as well as along-track ADCP velocity observations, were collected during June 2006, *R/V Oceanus* cruise OC425 (June 6–17, 2006) in the Gulf of Maine and Bay of Fundy (Fig. 1). The observations extended from near the coast to the 200-m isobath. In the current study, we focus on two transects conducted inside the Bay of Fundy (one in the central Bay, T3, and one near the mouth, T2) and another one just outside of the Bay, T1 (Fig. 2).

The observed depth-averaged velocity obtained from the ADCP (Fig. 2) has peak values of 0.8 ms^{-1} over the deeper part of the basin and 1.5 ms^{-1} over the shallow flanks of the western central Bay. The three-dimensional structure of the velocity is complex, with large vertical shear in the bottom and surface boundary layers and small shear in the mid-water column due to the action of the strong tide. In Fig. 2, depth-averaged velocity is used as an indication of tidal phase and horizontal shear in velocity. The observed velocities show the data collection inside the Bay included both

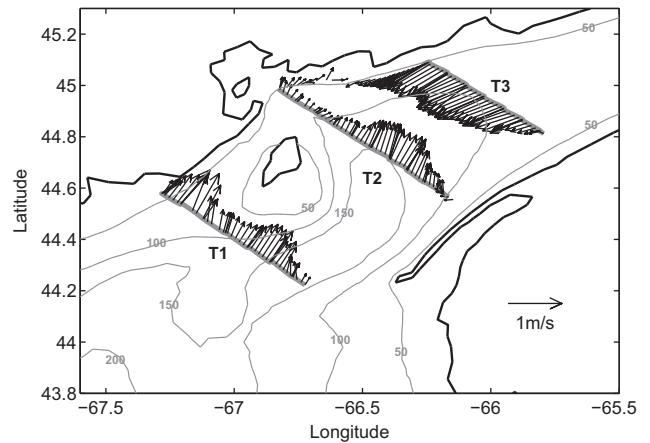


Fig. 2. Observed (ADCP) depth-averaged velocity in the proximity of the Bay of Fundy. The three transects conducted in (or in the proximity of) the Bay have been labeled: (T1), just outside the Bay in the northwestern Gulf of Maine; (T2), near the mouth of the Bay; and (T3), across the central Bay. Bottom topography contours of 50, 100, 150, and 200 m are indicated.

phases of the tide, with the transect in the central Bay (T3) sampled predominantly during ebb and the transect nearest the mouth (T2) occurring during flood. The data were collected during peak spring tides.

The reference temperature and salinity used as background conditions are specified from the Gulf of Maine climatology described in Lynch et al. (1996). These climatological fields have been successfully used in several previous studies of the Gulf of Maine and Bay of Fundy circulation (Lynch et al., 1997; He et al., 2005; Aretxabaleta et al., 2008).

3. Estimating initial model hydrography

3.1. General theory

Following the notation by Ide et al. (1997), consider a 3D primitive equation model $M(\mathbf{x}, \gamma)$, where in this case $\mathbf{x} = (S, T)$ is the (column) vector representing hydrography and γ are the remaining parameters of the model. The initial hydrography is $\mathbf{x}_0 = [S_0, T_0]$, where T_0 is the initial temperature field and S_0 is the initial salinity. In this notation, the subscript $_0$ refers to fields at the initial time. We can introduce a penalty function, $J = -2\log(L([S_0, T_0]|\mathbf{y}^o))$ (where L is the likelihood) which penalizes misfit to the data (\mathbf{y}^o , observations) and departures from climatology (\mathbf{x}_c):

$$J = (\mathbf{y}^o - \mathbf{H}M(\mathbf{x}_0, \gamma))^T \mathbf{R}^{-1} (\mathbf{y}^o - \mathbf{H}M(\mathbf{x}_0, \gamma)) + (\mathbf{x}_0 - \mathbf{x}_c)^T \mathbf{P}_0^{-1} (\mathbf{x}_0 - \mathbf{x}_c). \quad (1)$$

Here, \mathbf{R} is the observational error covariance matrix, \mathbf{H} is the measurement operator that, in our case, is assumed to be linear, \mathbf{P} is the model error covariance matrix with \mathbf{P}_0 being its value for the initial condition, and \mathbf{x}_c is the climatological estimate of \mathbf{x}_0 . In the 4DVAR variational method (Bennett, 1992; Wunsch, 1996) one seeks to minimize J as a function of \mathbf{x}_0 . For a general nonlinear model, M , constructing the solution that minimizes J can be challenging and computationally expensive. An alternative approach is to assume that the optimal estimate of \mathbf{x}_0 is a linear function of the misfit between the model and data, leading to Gauss-Markov smoothing. Bold characters represent linear operators, following Ide et al. (1997). It is easy to show that minimizing J with respect to \mathbf{x}_0 is solved by:

$$\hat{\mathbf{x}}_0 \mathbf{x}_c + \mathbf{A}_0 \mathbf{P} \mathbf{H}^T (\mathbf{H} \mathbf{P} \mathbf{H}^T + \mathbf{R})^{-1} (\mathbf{y}^o - \mathbf{H}M(\mathbf{x}_c, \gamma)), \quad (2)$$

where \mathbf{A}_0 is the matrix projecting the full space–time model vector onto the initial time point. The matrix \mathbf{P} represents the full space–time model error covariance matrix. Typically simplifications (e.g., Monte Carlo approximations) of this matrix are made, however for a 3D primitive equation model even this approach can be numerically expensive. Herein, we assume that \mathbf{P}_0 corresponds to the error covariance of the climatological fields ($\mathbf{P}_0 = \mathbf{P}_c$).

To avoid these computational burdens, time and the dynamic evolution of T and S can be ignored, leading to the penalty function of static fields (3DVAR):

$$J = (\mathbf{y}^o - \mathbf{H}_0\mathbf{x}_0)^T \mathbf{R}^{-1} (\mathbf{y}^o - \mathbf{H}_0\mathbf{x}_0) + (\mathbf{x}_0 - \mathbf{x}_c)^T \mathbf{P}_0^{-1} (\mathbf{x}_0 - \mathbf{x}_c). \quad (3)$$

Here \mathbf{H}_0 represents the measurement operator \mathbf{H} without the temporal component. Then:

$$\widehat{\mathbf{x}}_0 = \mathbf{x}_c + \mathbf{P}_0 \mathbf{H}_0^T (\mathbf{H}_0 \mathbf{P}_0 \mathbf{H}_0^T + \mathbf{R})^{-1} (\mathbf{y}^o - \mathbf{H}_0 \mathbf{x}_c). \quad (4)$$

3.2. Objective analysis

In this study, we refer to Objective Analysis (OA) as the particular form of statistical interpolation also commonly referred to as Optimal Interpolation (Lorenz, 1981, 1986). The OA method requires the specification of the two covariance functions (\mathbf{R} and \mathbf{P}_0) to compute the vector of optimal linear weights, λ^j , for the interpolation to node j :

$$\widehat{\mathbf{x}}^j = \mathbf{x}^j + \lambda^j \cdot (\mathbf{y}^o - \mathbf{H}_0 \mathbf{x}), \quad (5)$$

where

$$\lambda^j = \mathbf{P}_0^j \mathbf{H}_0^T (\mathbf{H}_0 \mathbf{P}_0 \mathbf{H}_0^T + \mathbf{R})^{-1}. \quad (6)$$

In OA, the model error covariance, \mathbf{P}_0 , is usually further simplified (Ghil and Malanotte-Rizzoli, 1991; Ide et al., 1997) by an approximate error covariance, \mathbf{B} , that includes the variances (empirical) in a diagonal matrix, \mathbf{D} , and the time-independent correlations, \mathbf{C} .

$$\mathbf{B} = \mathbf{D}^{1/2} \mathbf{C} \mathbf{D}^{1/2}. \quad (7)$$

After these approximations, the resulting weights are:

$$\lambda^j = \mathbf{B}_0^j \mathbf{H}_0^T (\mathbf{H}_0 \mathbf{B}_0 \mathbf{H}_0^T + \mathbf{R})^{-1}. \quad (8)$$

Statistical interpolation of oceanic data using objective analysis has been extensively described in the literature (Bretherton et al., 1976; Denman and Freeland, 1985; Wunsch, 1996). Several studies in the Gulf of Maine have used OA to estimate hydrographic and biological fields (Lynch et al., 1996; McGillicuddy et al., 1998; Lynch and McGillicuddy, 2001). A recent implementation of the OA method, called OACI (Objective Analysis for Circulation Initialization, Smith (2004)) has been successfully used for model initialization (He et al., 2005; Aretxabaleta et al., 2009). The approach consists of a simple implementation of a four-dimensional objective analysis method (Cressie, 1993). The software interpolates the residual (data to be interpolated minus background estimate of 3D field) onto any regular or irregular grid. The algorithm allows for the two configurations described in Cressie (1993) depending on the availability and quality of the background estimate: (1) simple kriging, assuming a zero mean; and (2) ordinary kriging, which assumes an unknown mean that is estimated during the procedure. For the rest of this study, we called this method “traditional objective analysis.”

3.3. An iterative approach

For the present goal of inferring initial conditions from a non-synoptic ($t_1 \leq t \leq t_2$) survey, the procedure produces one initial condition for $t = t_0$ by assuming the observations were nearly synoptic, $t \sim t_0$. We partly reintroduce the influence of the remaining parameters of the primitive equation model in Eq. (4) by computing

$$\widehat{\mathbf{x}}_0 = \mathbf{x}_c + \mathbf{P}_0 \mathbf{H}_0^T (\mathbf{H}_0 \mathbf{P}_0 \mathbf{H}_0^T + \mathbf{R})^{-1} (\mathbf{y}^o - \mathbf{H} \mathbf{M}(\mathbf{x}_c, \gamma)). \quad (9)$$

In this expression the model, M , remains non-linear instead of the previous linearization used for the traditional objective analysis (Section 3.2).

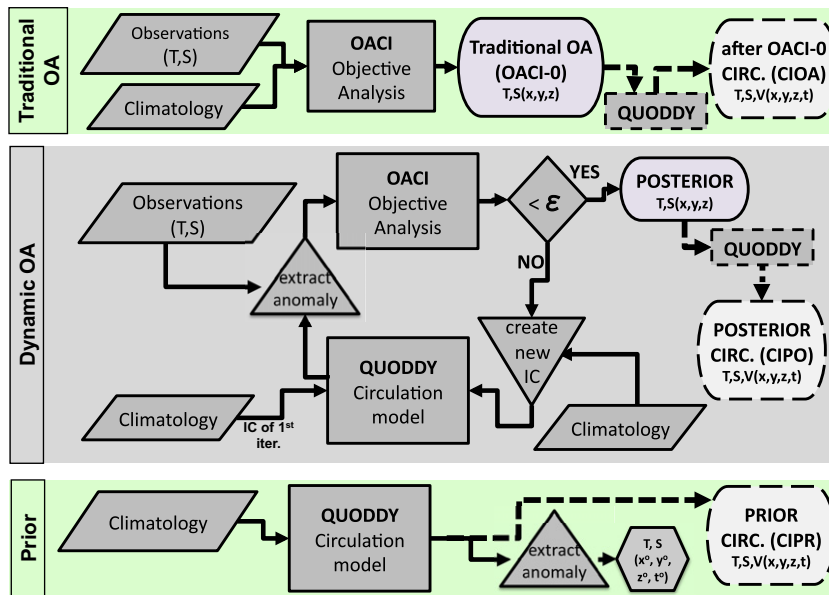


Fig. 3. Schematic diagram of the procedure followed. The top box corresponds to the traditional OA approach, which produces 3D (for all positions, x,y,z) hydrographic initialization fields (OACI-0) and, after going through the circulation model, results in 4D (all positions and times in the simulation, x,y,z,t) flow called CIOA. The bottom box represents the single pass through the circulation model initialized from climatology, that results in the prior 4D (x,y,z,t) flow (CIPR) and the anomaly extracted at the location of the observations (only for x^o,y^o,z^o,t^o). The central box corresponds to the iterative dynamical objective analysis. A decision is made to terminate the iterations when the global change in the hydrographic 3D field between successive iterations is less than a threshold ($\epsilon = 0.05$). If the threshold is not satisfied, a new set of initial conditions is generated that combine the climatology with the new 3D hydrographic fields. When the threshold is satisfied, a final pass through the circulation model produces the 4D flow field (CIPO). Dashed lines represent additional circulation model simulations and their output.

We now can create an iterative version, where $\mathbf{x}_0^j \mathbf{x}_c$, so that the non-linear effects of the model are reintroduced in our prediction,

$$\mathbf{x}_0^{j+1} = \mathbf{x}_0^j + \mathbf{P}_0 \mathbf{H}_0^T (\mathbf{H}_0 \mathbf{P}_0 \mathbf{H}_0^T + \mathbf{R})^{-1} (\mathbf{y}^o - \mathbf{H} \mathbf{M}(\mathbf{x}_0^j, \gamma)). \quad (10)$$

\mathbf{P}_0 remains constant through the iterations of the method. In general the model covariance matrix could present small deviations from the background (initial) model covariance, but in our method the assumption is the deviations are negligible.

The iterative OA approach can be simplified to a traditional OA component and a non-linear dynamic component. Our iterative dynamic OA method (Fig. 3) consists of five steps: (1) a circulation simulation initialized with climatological fields (same as prior simulation to be described in Section 3.4); (2) computation of the anomalies between observations and model fields; (3) objective analysis of the anomalies (using OACI, Smith (2004)); (4) adjustment of the initial conditions of the model with the objectively analyzed anomalies; (5) a circulation simulation using the updated initial conditions. Steps 2–5 are iterated to achieve convergence. In the application described herein, three iterations were sufficient to achieve convergence (less than 5% change between successive anomaly estimates). A similar approach without the iterative part has been previously described by Carton et al. (2000a) and Bennett (2002).

3.4. Oceanographic model

The primitive equation model “Quoddy” (Lynch and Werner, 1991) used herein has been extensively applied to the study of coastal circulation in the Gulf of Maine and adjacent areas (Lynch et al., 1996, 2001; Naimie, 1996; He et al., 2005). Quoddy is a three-dimensional, fully nonlinear, prognostic, tide-resolving, finite element model. To demonstrate the new analysis method, we apply it to a domain that includes most of the Gulf of Maine from Cape Cod to southwestern Nova Scotia and north up to the Bay of Fundy (Fig. 1). We focus our evaluation in the proximity of the Bay where tidal effects are especially strong. The finite element mesh includes fine horizontal resolution of 2–3 km near the coast increasing to around 8 km in the deep basins of the Gulf of Maine. Tidal forcing is included for five tidal constituents (M_2, S_2, N_2, O_1 , and K_1) using best estimates of the tidal boundary conditions (elevations and velocities) from climatological simulations (Lynch et al., 1996). Boundary conditions for temperature, salinity and residual elevation are also initialized from climatology (Lynch et al., 1996) but are updated to avoid inconsistencies at the boundary by using the interior values during times of outflow through the edge. Hourly wind stress from National Data Buoy Center (NDBC) station 44027 (Jonesport, ME) is enforced as surface boundary condition. Heat flux estimates are extracted from the NCEP/NCAR Reanalysis (Kalnay et al., 1996), while river discharge is obtained from US Geological Survey and Water Survey of Canada stream gauge stations. The circulation model is run for the duration of a cruise period during June 2006 plus an additional four days prior to the cruise to provide some spin-up time for initial and boundary conditions.

We refer to the first run of the circulation model (CIPR, initialized with climatology) as the “prior”, which does not include objective analysis for generation of initial condition. The final circulation simulation, after convergence is achieved through several OA/model iterations, is called the “posterior” circulation (CIPO). It is important to distinguish between the posterior hydrographic initial condition, valid for all discretized spatial locations at $t = t_0$, and the posterior circulation, valid for all discretized spatial locations and times.

4. Results and discussion

Five estimates of the hydrographic conditions during June 2006 can be constructed (Table 1) and their skill evaluated by comparison with observations:

- Climatological fields: assuming that the conditions during June 2006 matched the long-term mean.
- Traditional objective analysis (OACI-0): assuming the circulation can be neglected in the computation, i.e., all the observations during June 2006 are synoptic.
- Prior simulation: assuming the circulation model evolution of the climatological fields on short time scales can result in an appropriate representation of the real hydrographic structure (no assimilation of observations). Therefore it is equivalent to a hypothesis that the departures from climatology can be simulated by using realistic forcing on short time scales. This solution provides estimates of the field valid at the observation locations and times ($T, S(x^o, y^o, z^o, t^o)$), but not an initialization field (for $T, S(x, y, z)$ at $t = t_0$).

Table 1
Characteristics of the different hydrographic fields.

	Background	Observations	Circulation effects
Climatological	Climatology	Not included	NO
Traditional OA	Climatology	Included	NO
Prior analysis	Climatology	Not included	YES
1st Iter. analysis	Model prior	Included	YES
Posterior analysis	Model penult	Included	YES

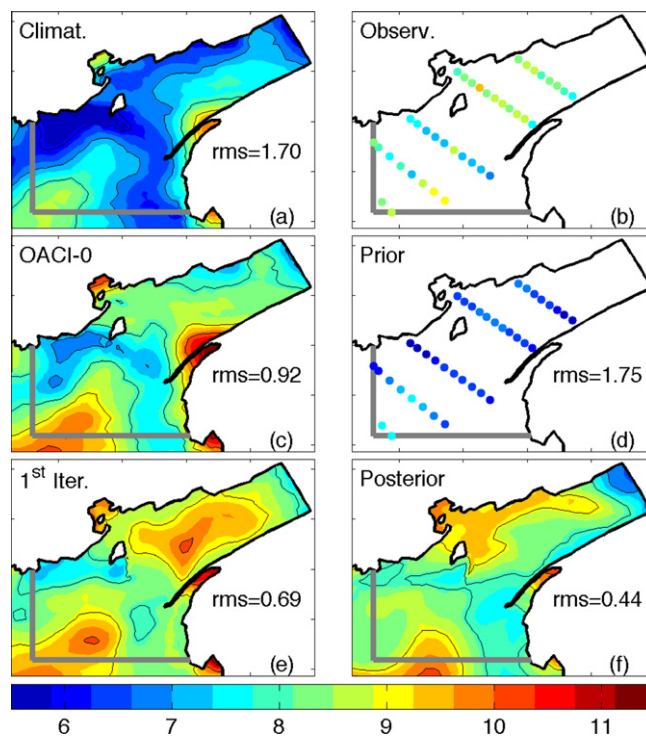


Fig. 4. Surface temperature (°C) estimates for different procedures and rms difference with observations. (a) Climatological, (b) observations, (c) simulation with no circulation adjustments (OACI-0), (d) prior estimate (one run of the circulation model), (e) field estimate after OA of observations into prior field (1st iteration), (f) posterior estimate (after the final iteration through the model procedure). The rms difference with observations inside the region indicated by the gray line is shown for each panel.

- First iteration analysis: projecting the observations into the anomalies calculated from the prior model simulation instead of the climatological fields.
- Posterior analysis: using the iterative dynamically adjusted objective analysis to provide an updated initial condition while considering the effects of circulation.

4.1. Model-data comparison

In this section an evaluation of the quality of the procedure is conducted by extracting, from the global 3D estimates, several sub-sampled fields: (1) surface temperature (SST); (2) vertical *T* and *S* profiles at specific locations; and (3) a vertical transect across the mouth of the Bay.

We extract the SST from the full 3D analysis to understand whether the method is able to recover the observed horizontal

spatial structure. The observed SST (Fig. 4b) is higher than climatology (Fig. 4a) in the northwestern Gulf of Maine and especially in the western Bay of Fundy (Root Mean Square (RMS) difference 1.7 °C). The observed SST hints at a southwest to northeast temperature gradient with higher values north of Grand Manan Island. The traditional objective analysis results in local corrections off Nova Scotia that are larger than necessary (Fig. 4c) but still reduces the difference with observations (RMS difference 0.9 °C). The surface temperature of the prior circulation solution (Fig. 4d) is a slight dynamical modification of the climatological field (RMS, 1.8 °C). The resulting changes introduced by the first iteration of the dynamic objective analysis (Fig. 4e) are more consistent with the observed values and produce a significant decrease in RMS difference (0.7 °C). In this case, the central part of the Bay near the gyre is modified too severely (due to large near-surface anomalies), resulting in higher than observed temperatures, that are resolved

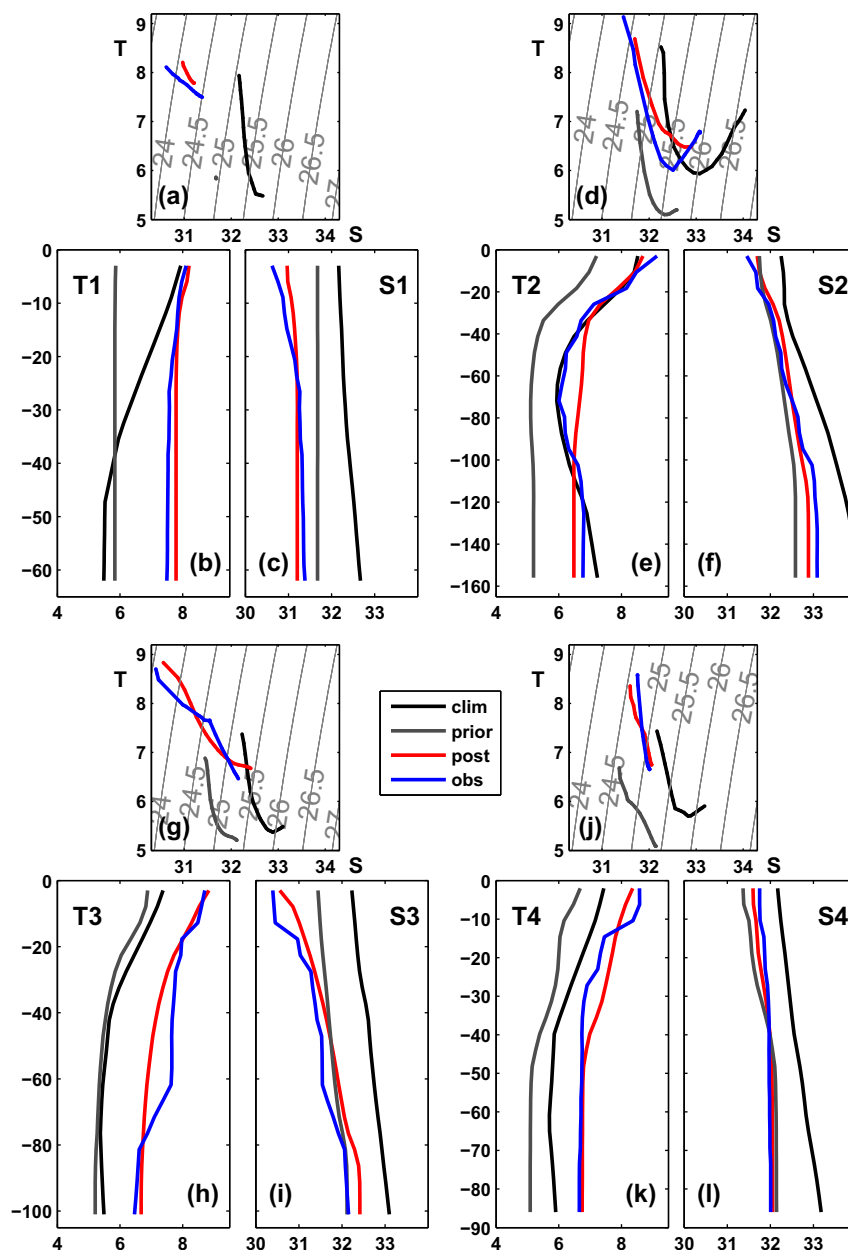


Fig. 5. *T/S* diagrams (a, d, g, j), temperature (b, e, h, k) and salinity (c, f, i, l) profiles at four selected locations in or near the Bay of Fundy (profile location in Fig. 1). Climatological values are represented with black lines, prior estimates with dark grey lines, posterior estimates with red and observed values with blue. Note that the prior *T/S* line is compressed to almost a point in panel a. (For interpretation of the references to colour in this figure legend, the reader is referred to the web version of this article.)

by the method in the following iteration. Surface temperature after the final iteration of the dynamical analysis (Fig. 4f) shows values (RMS 0.4 °C) and structures (reproduction of the large scale gradients) consistent with observations.

Modifications introduced by the dynamically adjusted objective analysis are more evident in the comparison of the changes of selected profiles (locations indicated in Fig. 1) between climatological background, observations, and dynamical estimates (Fig. 5). Each profile location represents a different dynamical regime within the Bay: profile 1 is outside the Bay and under the direct influence of the St. Croix river plume; profile 2 is in the center of the Bay of Fundy gyre (Aretxabaleta et al., 2009); profile 3 is directly affected by the St. John river plume; and profile 4 is near the axis of the Bay, outside the edge of the gyre. The climatological vertical temperature structure differs significantly (except for profile 2) from observations throughout the entire water column, with climatology being 1–2 °C colder in profiles 1, 3 and 4. The apparently parallel posterior and climatology temperature profiles for stations 3 and 4 present in fact differences ranging 0.8–1.5 °C. Meanwhile, the climatological salinity in these three profiles is 0.5–1 saltier than the observations. The observed hydrographic characteristics of profile 2 (Fig. 5d–f) are closer to climatological values, especially for temperature.

The *T/S* diagrams (Fig. 5a, d, g, j) demonstrate the ability of the method to reproduce the characteristics of the observations. The density differences shown by the *T/S* curves of the climatological and prior profiles illustrate significant inconsistencies with the observations. The posterior curves are considerably improved, and in general match the observed density variations. There are instances, such as the temperature in the middle of the water column from profile 2 (Fig. 5e), during which the model may have overestimated the tidal mixing resulting in reduced vertical gradients.

The stratification observed during June 2006 is generally stronger than the long-term average. The dynamic effect of the model

alone (prior) is the reduction of the climatological stratification caused by the strong tidal mixing in the Bay. Hence, the prior temperature profiles diverge even more from observations, while the prior salinity approaches the measured structure. Introduction of the dynamic objective analysis significantly improves the temperature and salinity match with observations, providing vertical stratification that is more realistic than the one present in the prior estimate. The corrections are larger for temperature, although corrections for salinity are significant in the areas downstream of the St. John and St. Croix river plumes (profiles 1 and 3, Fig. 5c, i).

Accurate representations of the hydrographic conditions inside the Bay of Fundy have been shown to be critical for the simulation of the circulation (Aretxabaleta et al., 2009). The intensity of the persistent gyre near the mouth of the Bay is strongly affected by the density structure, especially the dense water pool in the basin at the entrance of the Bay. To visualize the effect of the dynamic objective analysis on hydrographic structure, we examine a transect near the mouth of the Bay of Fundy (*T2*, Fig. 2). The observations (Fig. 6b) exhibit a strong low density signal in the north-western part of the transect resulting from the fresh water influence from the St. John river plume. High density values in the central part of the basin (50–150 m) are associated with the dense water pool. The climatological density across the mouth of the Bay is too high near the surface and too low in the lower part of the water column over the deep basin (Fig. 6a) compared with observations (Fig. 6b). Traditional objective analysis of the observations (Fig. 6c) results in a near-surface low density (salinity) plume with values lower than observed and an eastward displacement of the density maximum. The effect of the circulation model on the climatology (prior, Fig. 6d) is an increase of near-surface density from climatological values in the western side and an erosion of the deep density maximum. The first iteration (Fig. 6e) exhibits deep density values larger than observed. The near-surface effect of the St. John river plume and the increased density in the dense water pool are reproduced by the dynamical objective analysis procedure (Fig. 6f), with vertical stratification similar to observations.

4.2. Hydrographic skill

The global (three-dimensional) skill of the method is shown using histograms of the departure from observations (anomaly, Fig. 7), and evaluating bias, standard deviation, and RMS differences (Table 2). The observational error specified for the OA method (approximation to the **R** matrix) can be considered as a benchmark for the global skill. The values specified, 1.0 °C for temperature and 0.25 for salinity, are taken as approximations to the standard deviation of the difference between observations and the OA method without dynamic adjustments (OACI-0).

The climatological temperature (Fig. 7a, Table 2) has a large bias (1.5 °C) and standard deviation (1.6 °C). The traditional objective analysis (Fig. 7c) slightly reduces the bias in temperature (1.4 °C) and decreases the standard deviation. The fact that the bias is only slightly modified is the result of ordinary kriging (Cressie, 1993), which assumes an unknown mean that is estimated and removed during the procedure. The effect of just the circulation (prior) on temperature (Fig. 7e) is to decrease the standard deviation (0.9 °C) from the climatological initial condition while slightly increasing the bias. The first iteration of the dynamical OA method (Fig. 7g) results on the removal of most of the bias in temperature while producing a significant decrease in its standard deviation. The posterior estimate of temperature resulting from the dynamical method (Fig. 7i) reduces temperature bias (0.03 °C) and standard deviation (0.6 °C).

Climatological salinity (Fig. 7b, Table 2) is negatively biased (–0.4) with respect to observations and has a high standard

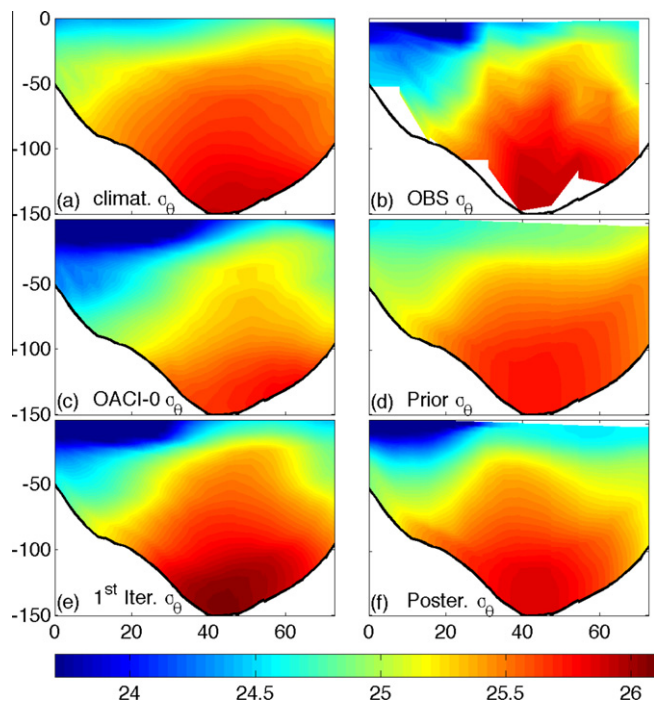


Fig. 6. Density transect (σ_θ) across the mouth of the Bay of Fundy (*T2* in Fig. 2). (a) Climatological, (b) observations, (c) traditional (OACI-0) objective analysis (no circulation) (d) prior estimate (after one pass through the circulation model, no observations), (e) first iteration of the dynamical OA (observations projected into the prior) and (f) posterior estimate (after the final pass through the dynamical analysis procedure). X-axis distance in km from the northwestern-most station in the transect (closest to New Brunswick).

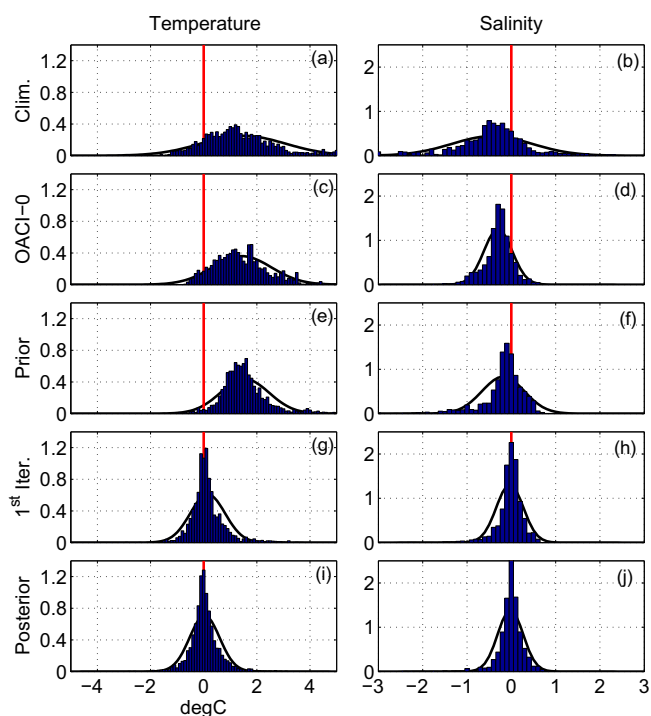


Fig. 7. Global skill evaluated as the departure from observations (anomaly) for temperature (left panels) and salinity (right panels). Climatological (a, b); traditional (OACI-0) objective analysis (c, d); prior, before OA (e, f); after the first (g, h) iteration of the dynamical objective analysis; and, finally, posterior dynamical objective analysis (i, j) probability density functions are presented (blue histograms). The normal probability density function with the same mean and standard deviation is presented for reference (black curve). Statistical values for bias, standard deviation and RMS difference for these distributions are given in Table 2.

Table 2

Global skill statistics corresponding to the histograms in Fig. 7 evaluated as the departure from observations (anomaly) for temperature and salinity. The bias, standard deviation, and RMS difference are calculated for each method and field.

	Temperature			Salinity		
	Bias	Std.	rms	Bias	Std.	RMS
Climat.	1.49	1.59	2.18	−0.43	0.91	1.01
OACI-0	1.44	1.11	1.82	−0.30	0.32	0.44
Prior	1.54	0.91	1.79	−0.18	0.48	0.51
1st Iter.	0.15	0.65	0.67	−0.03	0.30	0.31
Posterior	0.03	0.56	0.56	−0.02	0.29	0.29

deviation (0.9). The traditional objectively analyzed salinity (Fig. 7d) reduces the bias (−0.3) and decreases the standard deviation (0.3) by eliminating the large departures from observations. The prior salinity (Fig. 7f) shows a standard deviation reduction from climatological values (0.5) while decreasing the size of the bias by 60% from the climatological value. After objectively analyzing the observations into the prior (first iteration of the dynamical system, Fig. 7h) the bias is almost completely removed and the standard deviation is reduced from the prior values. The final iteration of the dynamically objectively analyzed salinity (Fig. 7j) maintains low bias (−0.02) while slightly reducing the standard deviation (0.3), resulting in RMS differences of the same order as the prescribed observational error.

4.3. Cross-validation analysis

In order to determine the robustness of the solution, we conduct a set of cross-validation experiments. We progressively

remove increasing numbers of stations (10–50% removal) at random from the analysis and repeat the experiment 100 times for each percentage. This approach represents a partial assimilation of the observations following a Monte Carlo approach allowing the comparison between removed observations and posterior estimates. We also conduct four additional experiments for which entire transects from the vicinity of the Bay of Fundy are systematically removed. The results of the analysis are determined with the metric given by

$$CV = \frac{rms[G(p_{extr})]}{rms[G^o(p_{extr})]}, \quad (11)$$

where G is the departure from observations of the hydrographic variables (temperature and salinity) for the posterior estimate evaluated at the stations removed from the analysis (p_{extr}) and G^o is the departure of that magnitude from the posterior analysis including all the stations evaluated at the same points (p_{extr}). For the extreme case of including all the stations, CV would have a value of 1.

The random removal of 10% of the data results in temperature and salinity fields qualitatively similar to the analysis using all the stations (not shown). The CV values (Table 3) are close to 1, which indicates that the method is robust and that the removal of a small percentage of the data does not deteriorate the solution significantly. Nevertheless, in some cases the removal of 10% of data from specific critical areas (e.g., near the mouth of the St. John river plume or near the central part of the gyre) is sufficient to produce a significant degradation of model performance locally. The progressive removal of more stations (20–50%) increases the difference from the original (best case) fields reaching CV values of 1.44 for temperature and 1.36 for salinity. The worst-case scenario in which all observations are removed (climatology) results in CV values larger than 3.5. The prior analysis (with all stations removed, no OA) produces CV values around 3. When single transects are systematically removed, the resulting fields show a significant worsening in CV values (larger than 2 for both T and S) even though they only represent 20–30% of the total data available in the Bay area. Removal of transects in the vicinity of the mouth to the Bay ($T1$ and $T2$ in Fig. 2) is especially damaging resulting in CV values that approach the worst-case scenario.

4.4. Dynamical implications

The focus herein has been on estimating the quality of the best estimates of the initialization fields based on a comparison between observed and objectively analyzed temperature and salinity. The requirements for the best initial conditions are not only that they should match the hydrographic observations but they should also provide the best skill for the circulation. The best estimate of the circulation for June 2006 comes from a hindcast (HC) study (Aretxabaleta et al., 2009) that focused on describing the characteristics and variability of the Bay of Fundy gyre. The June 2006 HC simulation used dynamic OA for initialization, but it differs from the simulations presented in the current study because it also used assimilation of shipboard ADCP velocities as well as current meters located at GOMOOS moorings A, B, E, I, J, L, and M (www.gomoo-

Table 3

Cross-validation results: average CV (Eq. (11)) for the 100 experiments for each percentage of station removal (10–50%). The column label transect is the average CV for the four transect removal experiments. The climatological (prior) CV values are calculated as the ratio between the hydrographic climatological (prior) values (i.e., all observations removed) and the posterior analysis including all stations.

	10%	20%	30%	40%	50%	Transect	Climat.	Prior
T	1.12	1.17	1.23	1.28	1.44	2.06	3.52	3.03
S	1.04	1.12	1.14	1.23	1.36	2.26	3.85	2.80

s.org). In the HC simulation, two different inverse models for velocity assimilation were used: a frequency-domain inversion to improve the model estimate of the tidal constituents and a time-domain adjoint to provide sub-tidal adjustments. A complete validation of the HC solution is available in Aretxabaleta et al. (2009). To summarize, the HC yielded hydrographic rms skill of 0.7 °C for temperature, 0.4 for salinity and circulation skill around 0.1 m s⁻¹ for the entire Gulf of Maine domain.

We use the HC as a benchmark for assessing the skill of the velocity predictions derived from the dynamic OA procedure. The time- and depth-averaged residual circulation for the period of the cruise from the HC simulation is presented in Fig. 8f.

The problem of comparing flows resulting from Quoddy simulations initialized from the fields described herein (e.g., CIPR, CIPO) with our benchmark HC is that Quoddy includes the effects of several factors (e.g., wind, density field, tides, river discharge, heat flux) that are not easily separated. In order to quantify the effects of the various initialization procedures on the density-driven flow, we calculated the steady-state residual circulation for each case by running a simplified circulation model (FUNDY5, Lynch and Werner (1987)). FUNDY5 is a linearized version of Quoddy in the frequency-domain that allows the separation of the different components of the circulation. FUNDY5 has been successfully applied in a number of coastal regimes (Lynch et al., 1992, 1996; Blanton et al., 2003; Ribergaard et al., 2004). The simplified circulation model uses the average mixing and friction from the time-domain solution to represent the effect of tidal mixing.

The steady-state circulation resulting from climatological density (Fig. 8a) is relatively weak, yet still includes a signature of the cyclonic gyre (Aretxabaleta et al., 2008). Traditional objective analysis results in unrealistic circulation features (Fig. 8b), such

Table 4

Circulation skill, in the proximity of the Bay, of Quoddy simulations initialized using the different hydrographic fields. The first row is the initialization field. The second row is the RMS size of difference (ms⁻¹) between model and observed velocities, except for the first column that corresponds to the size of the observed shipboard ADCP velocity. The HC value is italicized because these data were assimilated and thus the difference constitutes a metric of misfit rather than skill. The third row is the averaged separation rate (ms⁻¹) between observed and model drifters for the different model simulations. For the location of the drifter release, refer to Aretxabaleta et al. (2009). The last column corresponds to the hindcast results included in Aretxabaleta et al. (2009).

IC	Observ.	CIOA OACI-0	CIPR Climat.	CI1st 1st Iter.	CIPO Posterior	HC Posterior
ADCP	0.551	0.159	0.157	0.152	0.147	<i>0.134</i>
Drifters	0.385	0.088	0.088	0.082	0.079	0.078

as an anticyclonic circulation in the Bay and a strong outflow west of Grand Manan. We believe the inconsistent circulation results from tidal aliasing and a lack of a dynamical constraint. The depth-averaged circulation associated with the dynamically evolved climatological fields (prior, Fig. 8c) results in the recovery of the climatological structure of the gyre and the adjacent north-western Gulf of Maine circulation, but underestimates the strength of the gyre when compared with the reference hindcast simulation (Fig. 8f). The circulation associated with the hydrographic fields from the first iteration of the dynamic OA (Fig. 8d) exhibits a gyre that is stronger than in the hindcast, extending farther into the Bay. The steady-state circulation response to the posterior density field (Fig. 8e) exhibits similar features, consistent with the observed intensification of the gyre (Fig. 8f) during June 2006 (Aretxabaleta et al., 2009).

The preceding provides qualitative assessment of the time-averaged velocity field. In order to compute the differences between predicted and observed velocities in the time domain, the final forward Quoddy simulation is needed (Fig. 3, CIOA, CIPR, CIPO). This final simulation allows quantification of skill (Table 4) with regard to not only ADCP velocities (Fig. 2), but also from drifter trajectories. Nine drifters were released along the transect T2 across the Bay of Fundy as part of a multi-year Lagrangian study of the Gulf of Maine (Manning et al., 2009). The differences between observed and modeled trajectories are expressed as a velocity error that represents the mean rate of separation between simulated and observed drifters providing an integrated measure of skill for short period of times (0.5–2 days). The drifter-derived velocities were not assimilated in the HC simulation (Aretxabaleta et al., 2009) or in our current experiments. This skill metric is again compared with the benchmark provided by the fully assimilative hindcast simulation.

The difference between modeled and observed velocities decreases slightly from CIPR (Quoddy initialized with climatology) to the initialization from the first iteration product; a further reduction is achieved using the posterior as initialization (CIPO). The iterative procedure reduces the difference between the simulation initialized with the traditional OA (CIOA) and the reference hindcast (HC) simulation by 50%. Similar improvement is evident when the skill is estimated in terms of drifter separation rate. Of course, we do not expect CIPO to match the ADCP observations as much as the HC does, as these data were assimilated into the latter. Interestingly, CIPO exhibits skill comparable to the HC in terms of the drifter observations.

5. Conclusions

Dynamical evaluation of anomalies is presented as an alternative to traditional objective analysis methods for the generation of initialization of short-term hindcast/forecast simulations. The method is much faster and computationally less expensive than

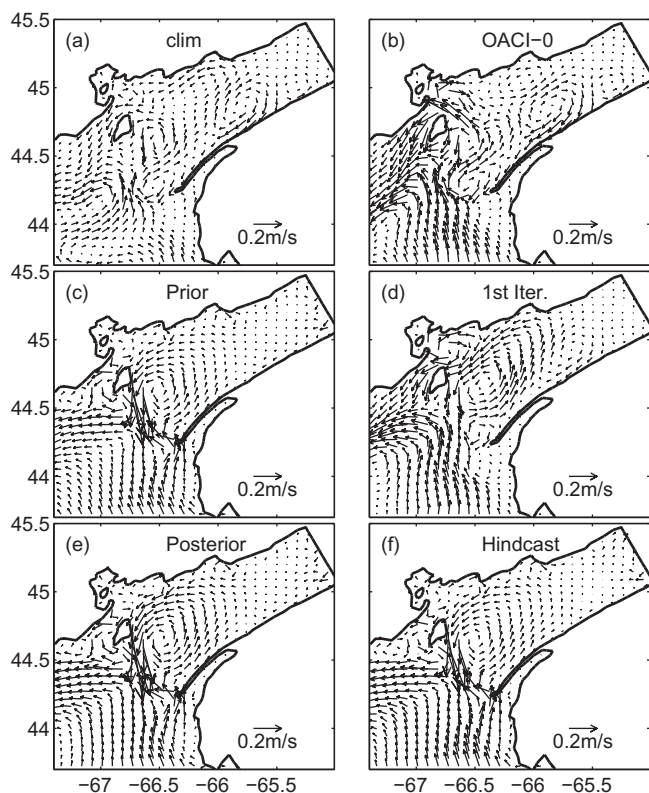


Fig. 8. Residual steady-state response (depth-averaged velocity) to the density fields calculated with the different methods using the frequency-domain linear model FUNDY5: (a) Climatological response, (b) traditional objective analysis, (c) prior (no OA), (d) first iteration, and (e) posterior estimates. The averaged flow during the cruise period computed in the hindcast simulation (Aretxabaleta et al., 2009) is included in panel (f).

other data assimilation procedures such as ensemble methods (3–4 circulation model runs in our method versus normal ensemble sizes requiring 50–100 members).

In this application, dynamical objective analysis reduced both temperature and salinity biases to near-zero values. In addition, standard deviations of the misfits were significantly reduced. We hypothesize that these improvements are attributed primarily to the correction of tidal aliasing of observations in the Bay. The resulting circulation exhibits skill approaching that of a hindcast simulation that includes both hydrographic and velocity data assimilation (Aretxabaleta et al., 2009). We expect the dynamical objective analysis procedure described herein to be particularly useful in regions of large tidal amplitude and/or in the proximity of sharp gradients such as fronts.

Acknowledgments

The preparation of this paper was supported by NSF/NIEHS Grant OCE-0430724 (Woods Hole Center for Oceans and Human Health) and NOAA Grant NA06NOS4780245 (GOMTOX). The authors want to thank the crew of R/V Oceanus for their assistance during the cruise. A. Aretxabaleta has been additionally supported by I3P and Juan de la Cierva grants of the Spanish Government.

References

- Aretxabaleta, A.L., McGillicuddy, D.J., Smith, K.W., Lynch, D.R., 2008. Model simulations of the Bay of Fundy gyre: 1. Climatological results. *J. Geophys. Res.* 113 (C10027). doi:10.1029/2007JC004480.
- Aretxabaleta, A.L., McGillicuddy, D.J., Smith, K.W., Manning, J.P., Lynch, D.R., 2009. Model simulations of the Bay of Fundy gyre: 2. Hindcasts for 2005–2007 reveal interannual variability in retentiveness. *J. Geophys. Res.* 114 (C09005). doi:10.1029/2008JC004948.
- Ballabrera-Poy, J., Busalacchi, A.J., Murtugudde, R., 2001. Application of a reduced order Kalman filter to initialize a coupled atmosphere-ocean model. Impact on the prediction of El Niño. *J. Climate* 14, 1720–1737.
- Bennett, A.F., 1992. *Inverse Methods in Physical Oceanography*. Cambridge University Press. pp. 346.
- Bennett, A.F., 2002. *Inverse Modeling of the Ocean and Atmosphere*. Cambridge University Press. pp. 234.
- Bigelow, H.B., 1927. Physical oceanography of the Gulf of Maine. *Bull. US Bur. Fish.* 49, 511–1027.
- Bisagni, J.J., Gifford, D.J., Ruhsam, C.M., 1996. The spatial and temporal distribution of the Maine Coastal Current during 1982. *Cont. Shelf Res.* 16, 1–24.
- Blanton, B.O., Aretxabaleta, A.L., Werner, F.E., Seim, H., 2003. Monthly climatology of the continental shelf waters of the South Atlantic Bight. *J. Geophys. Res.* 108 (C8). doi:10.1029/2002JC001609.
- Bretherton, F.P., Davis, R.E., Fandry, C.B., 1976. A technique for objective analysis and design of oceanographic experiments applied to MODE-73. *Deep-Sea Res.* 23, 559–582.
- Brooks, D.A., 1985. Vernal circulation of the Gulf of Maine. *J. Geophys. Res.* 90 (C3), 4687–4705.
- Brooks, D.A., 1994. A model study of the buoyancy-driven circulation in the Gulf of Maine. *J. Phys. Oceanogr.* 24, 2387–2412.
- Brooks, D.A., Townsend, D.W., 1989. Variability of the coastal current and nutrient pathways in the eastern Gulf of Maine. *J. Marine Res.* 47, 303–321.
- Carton, J.A., Chepurin, G., Cao, X., 2000a. A simple ocean data assimilation analysis of the global upper ocean 1950–1995. Part I: Methodology. *J. Phys. Oceanogr.* 30, 294–309.
- Carton, J.A., Chepurin, G., Cao, X., 2000b. A simple ocean data assimilation analysis of the global upper ocean 1950–1995. Part II: Results. *J. Phys. Oceanogr.* 30, 311–326.
- Cressie, N.A.C., 1993. *Statistics for Spatial Data*. Wiley Series in Probability and applied Mathematics. Wiley.
- Danabasoglu, G., McWilliams, J.C., Large, W.G., 1996. Approach to equilibrium in accelerated global oceanic models. *J. Climate* 9, 1092–1110.
- Denman, K.L., Freeland, H.J., 1985. Correlation scales, objective mapping and a statistical test of geostrophy over the continental shelf. *J. Marine Res.* 43, 517–539.
- Ezer, T., Mellor, G.L., 1994. Diagnostic and prognostic calculations of the north atlantic circulation and sea level using a sigma coordinate ocean model. *J. Geophys. Res.* 99 (14), 159–175.
- Fukumori, I., Benveniste, J., Wunsch, C., Haidvogel, D.B., 1993. Assimilation of sea surface topography into an ocean circulation model using a steady-state smoother. *J. Phys. Oceanogr.* 23, 1831–1855.
- Garrett, C.J.R., 1972. Tidal resonance in the Bay of Fundy and Gulf of Maine. *Nature* 238, 441–443.
- Ghil, M., Malanotte-Rizzoli, P., 1991. Data assimilation in meteorology and oceanography. *Adv. Geophys.* 33, 141–266.
- Goerss, J.S., Phoebus, P.A., 1993. The multivariate optimum interpolation analysis of meteorological data at the Fleet Numerical Oceanographic Center NRL/FR/7531-92-9413. Tech. rep., Naval Research Laboratory, Monterey, CA. pp. 58.
- Greenberg, D.A., 1983. Modeling the mean barotropic circulation in the Bay of Fundy and Gulf of Maine. *J. Phys. Oceanogr.* 13, 886–904.
- He, R., McGillicuddy, D.J., Lynch, D.R., Smith, K.W., Stock, C.A., Manning, J.P., 2005. Data assimilative hindcast of the Gulf of Maine Coastal Circulation. *J. Geophys. Res.* 110 (C10011). doi:10.1029/2004JC002807.
- Ide, K., Courtier, P., Ghil, M., Lorenc, A.C., 1997. Unified notation for data assimilation: operational, sequential and variational. *J. Met. Soc. Jpn.* 75, 181–189.
- Kalnay, E., Kanamitsu, M., Kistler, R., Collins, W., Deaven, D., Gandin, L., Iredell, M., Saha, S., White, G., Woollen, J., Zhu, Y., Leetmaa, A., Reynolds, R., Chelliah, M., Ebisuzaki, W., Higgins, W., Janowiak, J., Mo, K.C., Ropelewski, C., Wang, J., Jenne, R., Joseph, D., 1996. The NCEP/NCAR 40-year Reanalysis Project. *Bull. Amer. Met. Soc.* 77 (3), 437–471.
- Kleeman, R., Moore, A.M., Smith, N.R., 1995. Assimilation of subsurface thermal data into a simple ocean model for the initialisation of an intermediate tropical coupled ocean-atmosphere forecast model. *Mon. Wea. Rev.* 123, 3103–3113.
- Lorenc, A.C., 1981. A global three-dimensional multivariate statistical interpolation scheme. *Mon. Wea. Rev.* 109 (4), 701–721.
- Lorenc, A.C., 1986. Analysis methods for numerical weather prediction. *Q. J. R. Meteorol. Soc.* 112, 1177–1194.
- Lorenc, A.C., Ballard, S.P., Bell, R.S., Ingleby, N.B., Andrews, P.L.F., Barker, D.M., Bray, J.R., Clayton, A.M., Dalby, T., Li, D., Payne, T.J., Saunders, F.W., 2000. The Met. Office global three-dimensional variational data assimilation scheme. *Q.J.R. Meteorol. Soc.* 126, 2991–3012.
- Lynch, D.R., Holboke, M.J., Naimie, C.E., 1997. The Maine Coastal Current: Spring climatological circulation. *Cont. Shelf Res.* 17, 605–634.
- Lynch, D.R., Ip, J.T.C., Naimie, C.E., Werner, F.E., 1996. Comprehensive coastal circulation model with application to the Gulf of Maine. *Cont. Shelf Res.* 16, 875–906.
- Lynch, D.R., McGillicuddy, D.J., 2001. Objective analysis for coastal regimes. *Cont. Shelf Res.* 21, 1299–1315.
- Lynch, D.R., Naimie, C.E., Ip, J.T., Lewis, C.V., Werner, F.E., Luettich, R.A., Blanton, B.O., Quinlan, J.A., McGillicuddy, D.J., Ledwell, J.R., Churchill, J., Kosnyrev, V., Davis, C.S., Gallagher, S.M., Ashjian, C.J., Lough, R.G., Manning, J., Flagg, C.N., Gorman, C.G.H.R.C., 2001. Real-time data assimilative modeling on Georges Bank. *Oceanography* 14 (1), 65–77.
- Lynch, D.R., Werner, F.E., 1987. Three-dimensional hydrodynamics on finite elements. Part I: Linearized harmonic model. *Int. J. Numer. Methods Fluids* 7, 871–909.
- Lynch, D.R., Werner, F.E., 1991. Three-dimensional hydrodynamics on finite elements. Part II: Non-linear time-stepping model. *Int. J. Numer. Methods Fluids* 12, 507–533.
- Lynch, D.R., Werner, F.E., Greenberg, D.A., Loder, J.W., 1992. Diagnostic model for baroclinic, wind-driven and tidal circulation in shallow seas. *Cont. Shelf Res.* 1, 37–64.
- Malanotte-Rizzoli, P., Holland, W.R., 1986. Data constraints applied to models of the ocean general circulation. Part I: The steady case. *J. Phys. Oceanogr.* 16, 1665–1682.
- Manning, J.P., McGillicuddy, D.J., Pettigrew, N.R., Churchill, J.H., Incze, L.S., 2009. Drifter observations of the Gulf of Maine Coastal Current. *Cont. Shelf Res.* 29, 835–845.
- Marotzke, J., Wunsch, C., 1993. Finding the steady state of a general circulation model through data assimilation: application to the North Atlantic Ocean. *J. Geophys. Res.* 98, 20149–20167.
- McGillicuddy, D.J., Lynch, D.R., Moore, A.M., Gentleman, W.C., Davis, C.S., 1998. An adjoint data assimilation approach to the estimation of pseudocalanus spp. population dynamics in the Gulf of Maine-Georges Bank region. *Fisheries Oceanogr.* 7 (3–4), 205–218.
- McWilliams, J.C., 1996. Modeling the ocean general circulation. *Ann. Rev. Fluid Mech.* 28, 215–248.
- Naimie, C.E., 1996. Georges Bank residual circulation during weak and strong stratification periods: prognostic numerical model results. *J. Geophys. Res.* 101 (C3), 6469–6486.
- Ribergaard, M.H., Pedersen, S.A., Adlandsvik, B., Kliem, N., 2004. Modelling the ocean circulation on the West Greenland shelf with special emphasis on northern shrimp recruitment. *Cont. Shelf Res.* 24, 1505–1519.
- Robinson, A.R., Arango, H.G., Miller, A.J., Warn-Varnas, A., Poulain, P.M., Leslie, W.G., 1996. Real-time operational forecasting on shipboard of the Iceland-Faeroe frontal instability. *Bull. Amer. Met. Soc.* 77 (2), 243–259.
- Robinson, A.R., Span, M.A., Walstad, L.J., Leslie, W.G., 1989. Data assimilation and dynamical interpolation in gulfcast experiments. *Dyn. Atmos. Oceans* 13, 301–316.
- Smith, K.W., 2004. *Objective Analysis for Circulation Initialization (OACI) 1.2 users' guide*. Tech. rep., Numer. Model. Lab., Dartmouth College, Hanover, NH. Available at <<http://www-nml.dartmouth.edu/circmods/gom.html>>.
- Stammer, D., Davis, R., Fu, L.-L., Fukumori, I., Giering, R., Lee, T., Marotzke, J., Marshall, J., Menemenlis, D., Niiler, P., Wunsch, C., Zlotnicki, V., 2000. Ocean state estimation in support of CLIVAR and GODAE. *CLIVAR Exchanges* 5, 3–5. <www.clivar.org>.
- Wunsch, C., 1996. *The Ocean Circulation Inverse Problem*. Cambridge University Press. pp. 442.